

Supplementary Material

Development of Fluorescent Carbon Nanoparticle-Based Probes for Intracellular pH and Hypochlorite Sensing

Yu-Syuan Lin ¹, Li-Wei Chuang ¹, Yu-Feng Lin ¹, Shun-Ruei Hu ¹, Chih-Ching Huang ^{2,3,4}, Yu-Fen Huang ^{4,5,6,*} and Huan-Tsung Chang ^{1,*}

¹ Department of Chemistry, National Taiwan University, Taipei 10617, Taiwan;

hero1245337@gmail.com (Y.-S.L.); abcdony@gmail.com (L.-W.C.); assassin52852@gmail.com (Y.-F.L.);

ick20140216@gmail.com (S.-R.H.)

² Department of Bioscience and Biotechnology, National Taiwan Ocean University, Keelung 20224, Taiwan;

huangjing@mail.ntou.edu.tw

³ Center of Excellence for the Oceans, National Taiwan Ocean University, Keelung 20224, Taiwan

⁴ School of Pharmacy, College of Pharmacy, Kaohsiung Medical University, Kaohsiung 80708, Taiwan

⁵ Institute of Analytical and Environmental Sciences, National Tsing Hua University, Hsinchu 30013, Taiwan

⁶ Department of Biomedical Engineering and Environmental Sciences, National Tsing Hua University, Hsinchu 30013, Taiwan

* Correspondence: yufen@mx.nthu.edu.tw (Y.-F.H.); changht@ntu.edu.tw (H.-T.C.)

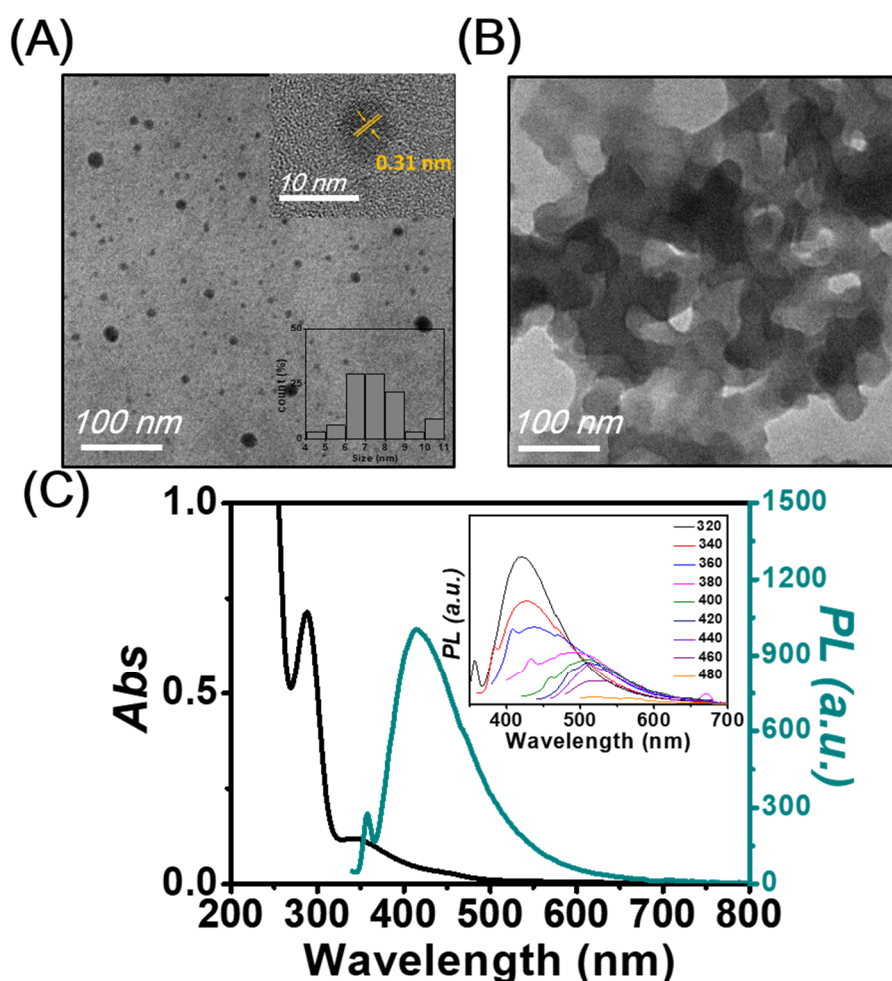


Figure S1. TEM images of (A) *m*-PD CDs (insets: high-resolution TEM image and size distribution analysis) and (B) AA nanoparticulates. (C) UV-Vis absorption and fluorescence spectra of *m*-PD CDs. Inset: fluorescence spectra of *m*-PD CDs in aqueous solution as a function of excitation wavelength.

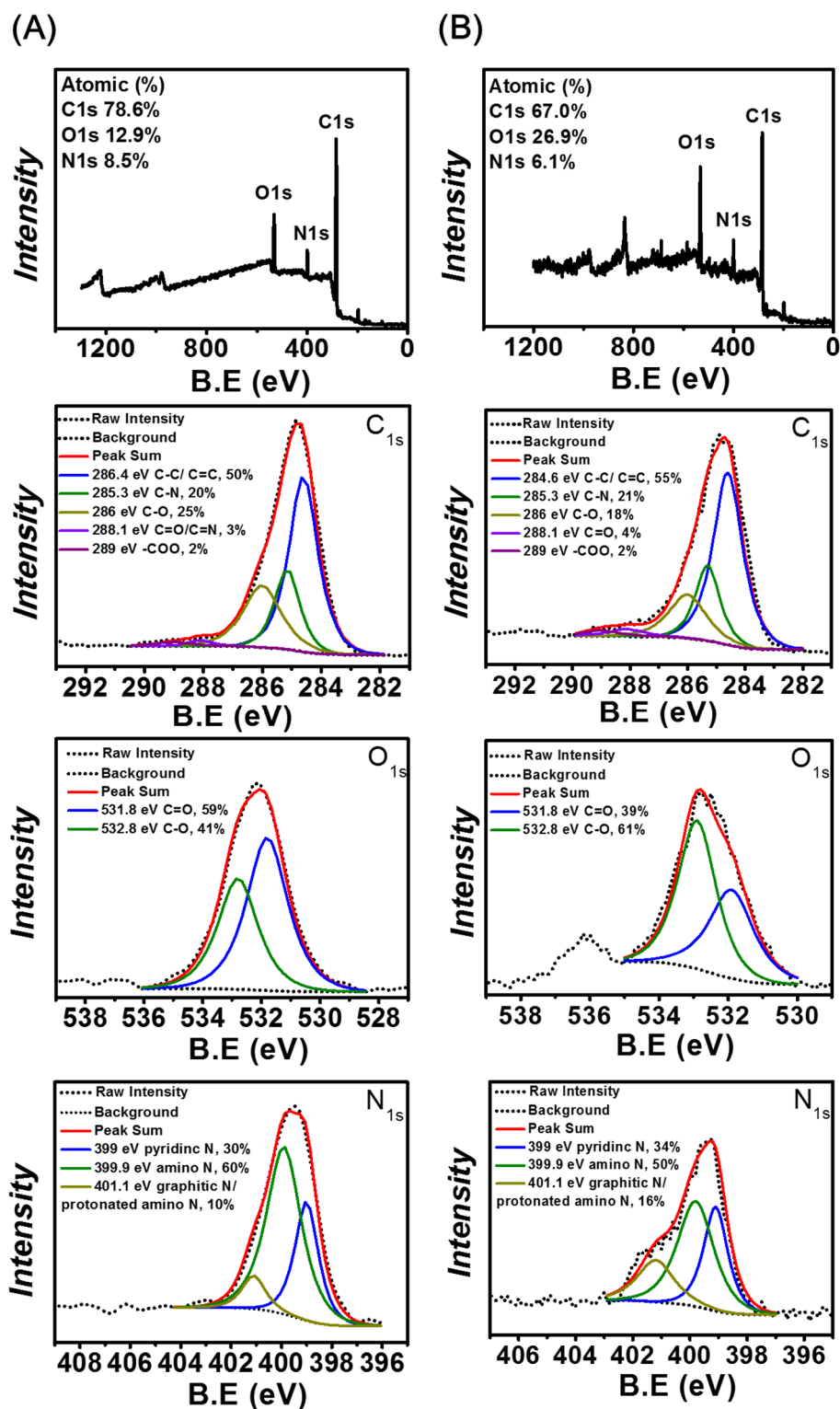


Figure S2. XPS survey spectra and high-resolution XPS scan spectra over C_{1s}, O_{1s} and N_{1s} of (A) mPA CNPs and (B) *m*-PD CDs.

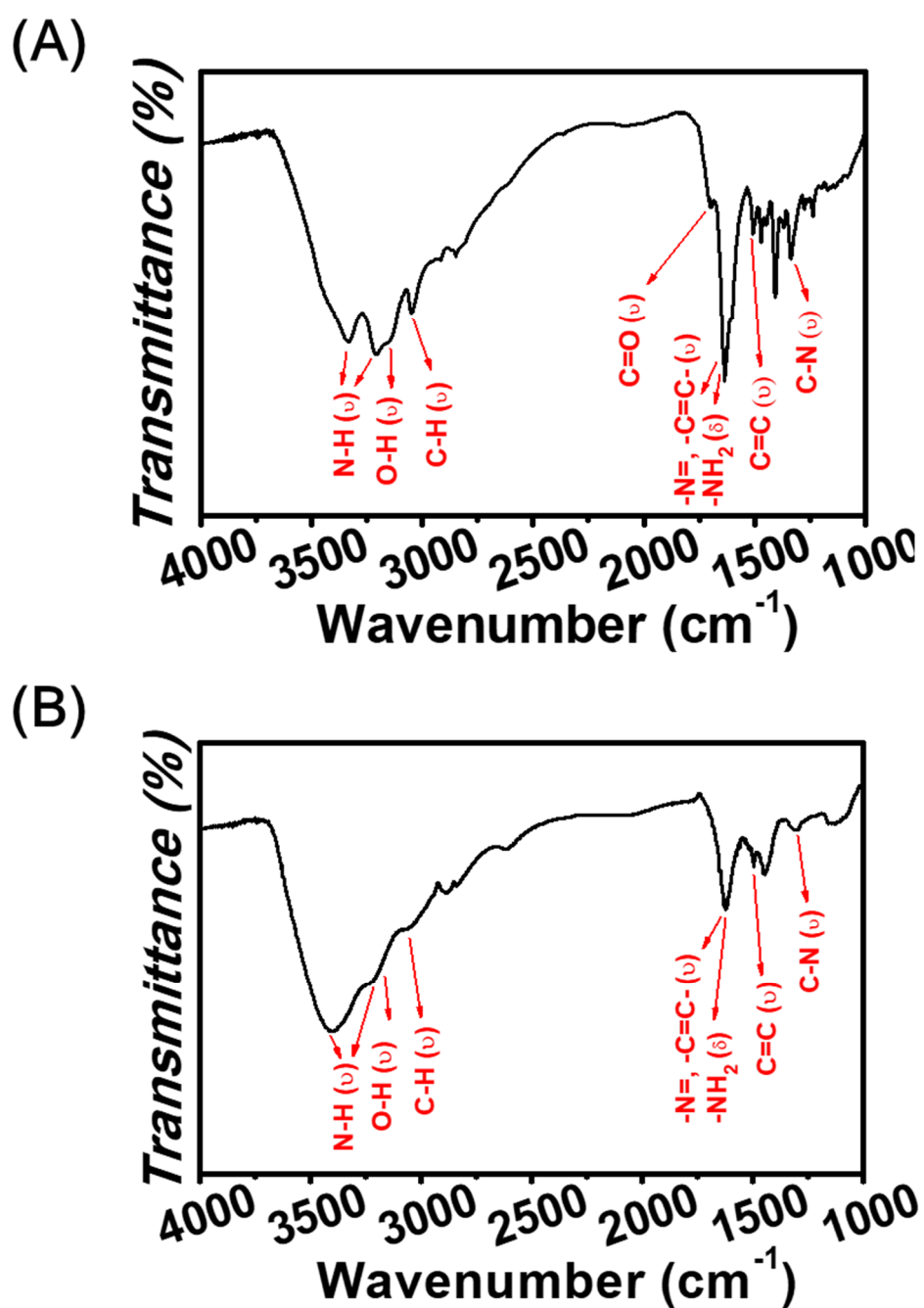


Figure S3. FT-IR spectra of (A) mPA CNPs and (B) *m*-PD CDs (ν : stretching, δ : bending).

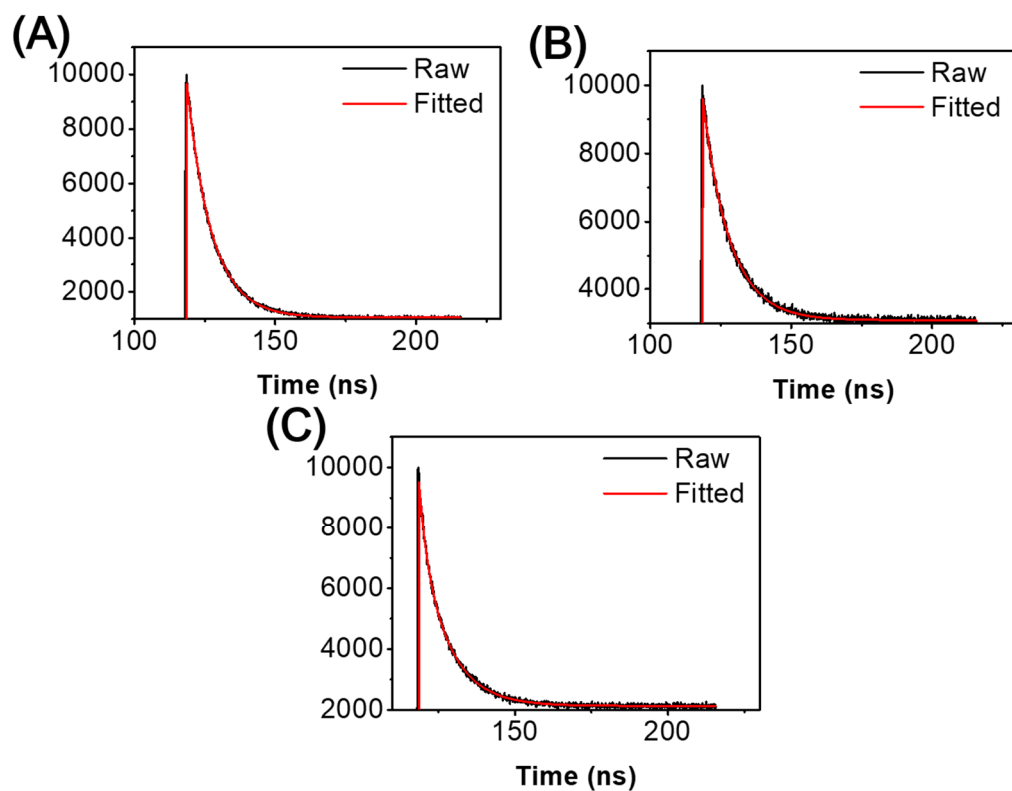
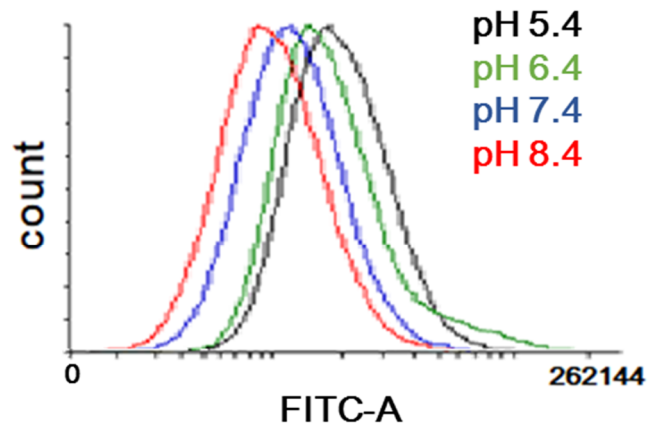


Figure S4. Fluorescence decay curves of mPA CNPs ($1.0 \mu\text{g mL}^{-1}$) at pH (A) 3.0, (B) 7.0 and, (C) 11.0 upon excitation using a 375-nm pulsed laser.

(A)



(B)

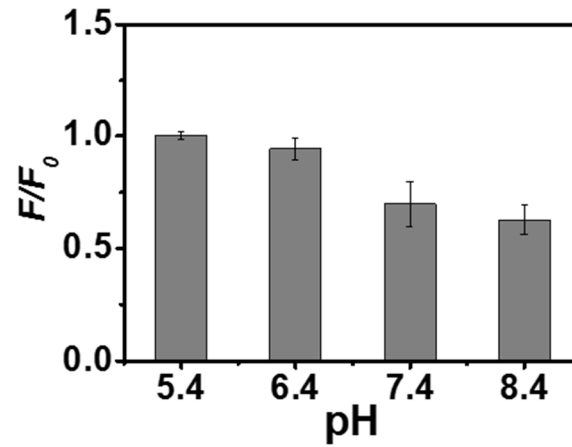


Figure S5. Flow cytometry analysis of Tramp C1 cells treated with mPA CNPs ($5 \mu\text{g mL}^{-1}$) at various pH values for 2 h. (A) A histogram (number of events versus FITC channel signal) and (B) The bar graph representing the relative fluorescence intensity (F/F_0) versus the pH value. F_0 and F denote the mean fluorescence intensities of mPA CNPs in Tramp C1 cells at pH 5.4 and other specific pH values, respectively.

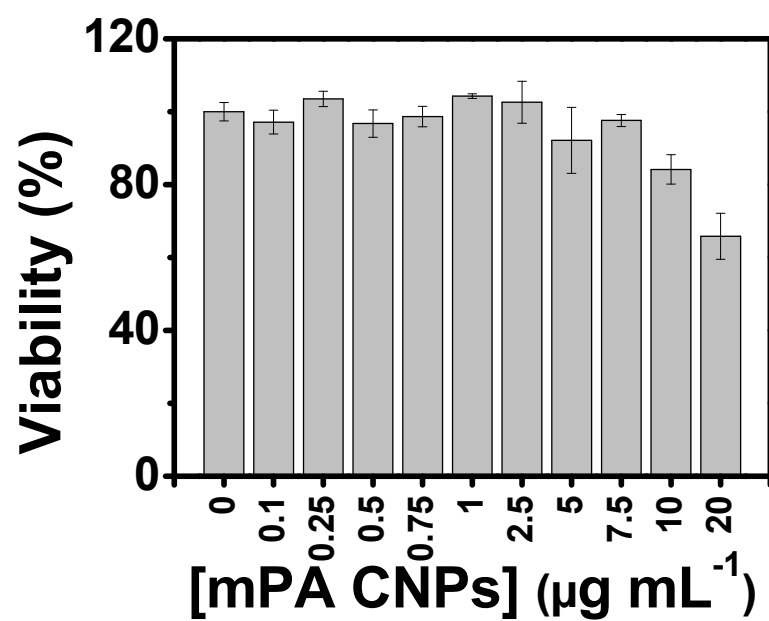


Figure S6. Cell viability for Tramp C1 cells in the presence of a series of concentrations of mPA CNPs.

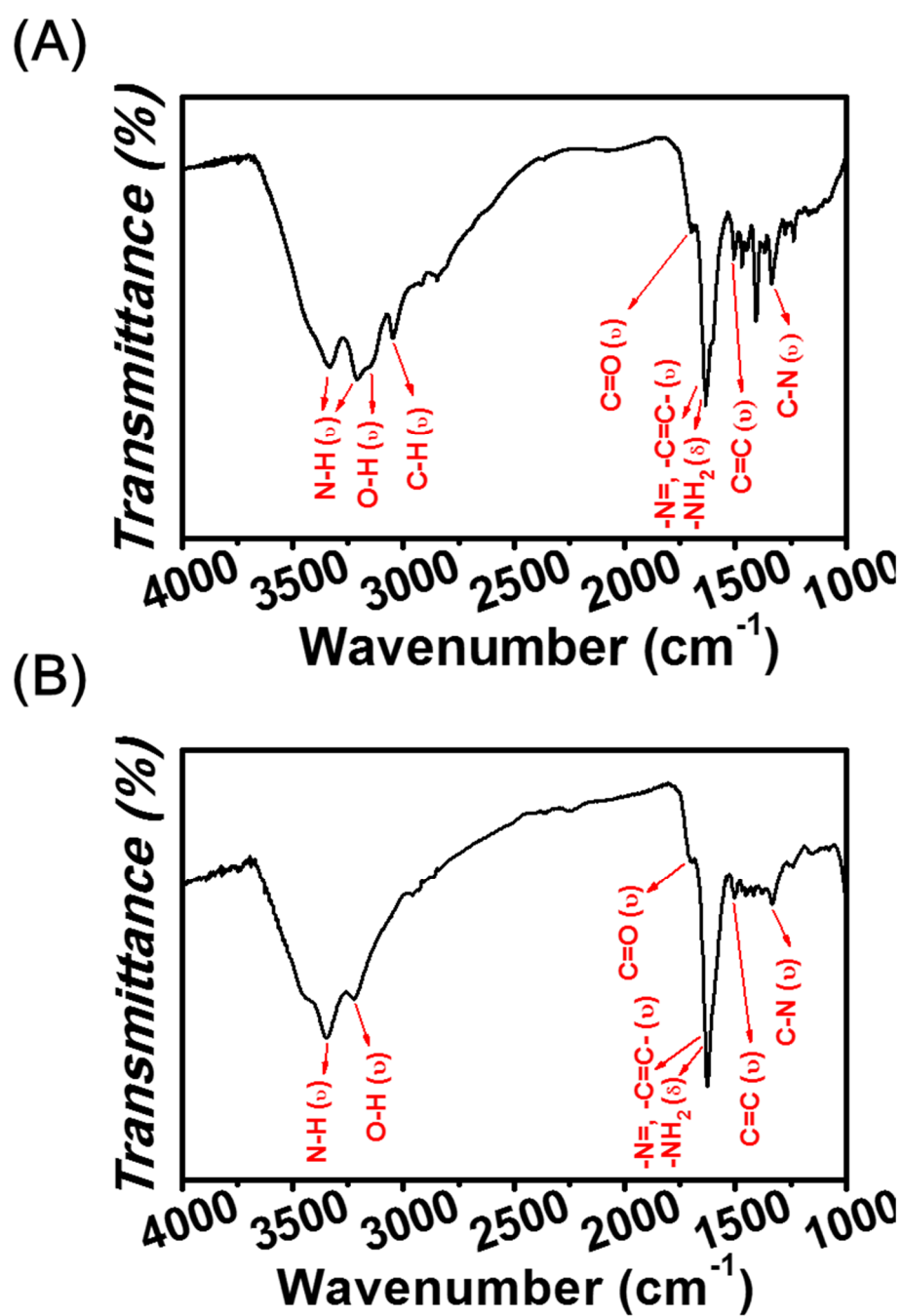


Figure S7. FT-IR spectra of mPA CNPs in the (A) absence and (B) presence of NaClO (100 μM).

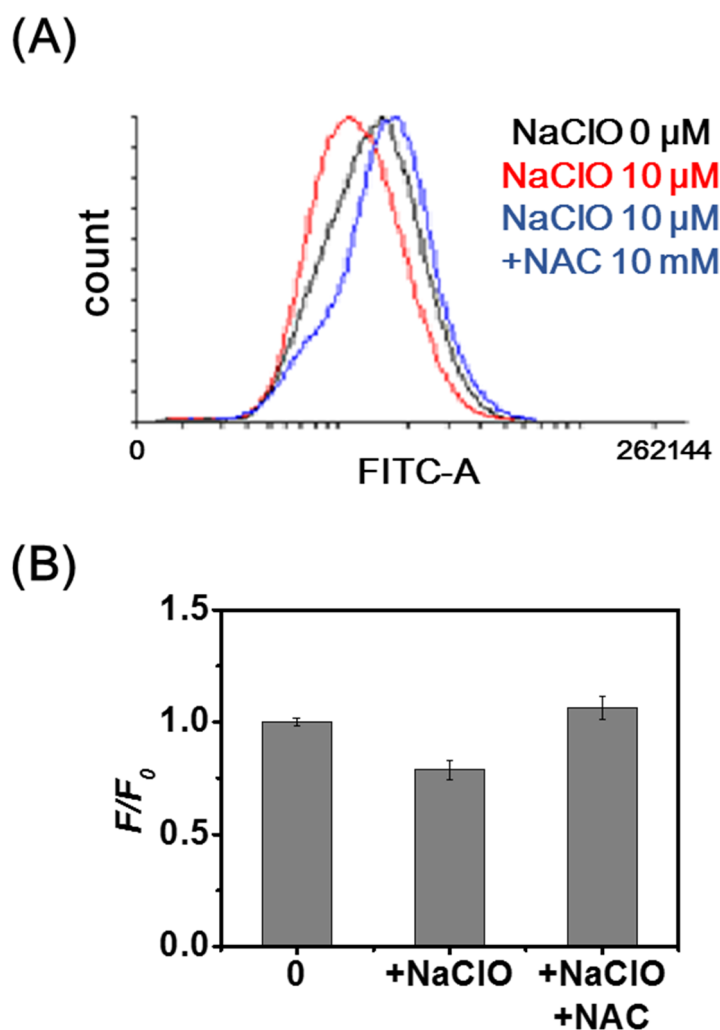


Figure S8. Flow cytometry analysis of Tramp C1 cells stained with mPA CNPs ($5 \mu\text{g mL}^{-1}$) incubated with NaClO ($10 \mu\text{M}$) or NaClO/NAC ($10 \mu\text{M}$ and 10 mM , respectively) for 30 min. (A) A histogram (number of events versus FITC channel signal) and (B) The bar graph representing the relative fluorescence intensity (F/F_0) versus different treatments. F_0 and F denote the mean fluorescence intensities of mPA CNPs in Tramp C1 cells in the absence and presence of hypochlorite.

Table S1. Zeta potentials of mPA CNPs ($1 \mu\text{g mL}^{-1}$) at various pH values.

pH	Zeta Potential (mV)
3.0	16.3 ± 1.3
5.0	11.7 ± 1.8
7.0	6.5 ± 0.6
9.0	-2.1 ± 1.5
11.0	-4.7 ± 1.4

Table S2. Comparison of the in vitro fluorescence behavior of mPA CNPs with other CD-based pH sensors.

Materials	Precursors	Linear pH Range	Dosage ($\mu\text{g mL}^{-1}$)	Labeling Time (h)	Reference
pH-CDs	<i>p</i> -phenylenediamine, <i>o</i> -phenylenediamine and dopamine	3.5–6.5	20	0.5	16
N-CDs	<i>p</i> -phenylenediamine	2.6–4.6; 5.0–6.8	600	0.5	38
CDs	anthranilic acid and <i>o</i> -phenylenediamine	3.0–8.0 (non-linear)	400	4	48
BNSCDs	4-carboxyphenyl-boronic acid and 2,5-diaminobenzenesul-fonic acid	1.6–7.0	500	0.5	49
Y-CDs	<i>o</i> -phenylenediamine	4.0–8.2	40	4	52
G-CDs	<i>m</i> -phenylenediamine	6–10	40	5	53
CDs	citric acid and basic fuchsin	5.2–8.8	500	2	54
mPA CNPs	<i>m</i> -phenylenediamine and ascorbic acid	5.5–8.5	5	2	This work

Table S3. Comparison of the fluorescence behavior of mPA CNPs with other CD-based hypochlorite sensors.

Materials	Precursors	Linear Range (μM)	LOD (nM)	Reference
CDs	ethanol and H_2O_2	0.1–10	80	24
CDs	3-aminophenylboronic acid and alizarin red S	0–200	4470	25
Cl ₂ N-CDs	dried shaddock peel and concentrated HCl	3.24–216	2880	26
GAAP-CDs	glutaric acid and 3-aminophenylboronic acid	0.1–100	500	27
N-CDs	neutral red and glutamine	1.5–112.5; 112.5–187.5	270	29
N, P-CDs	safranin T and phosphoric acid	0.74–5.93; 5.93–25.93	46.1	31
RD-CDs	2,5-diaminobenzenesulfonic acid	0.1–100	83	55
mPA CNPs	<i>m</i> -phenylenediamine and ascorbic acid	0.125–1.25	29	This work

Table S4. One electron redox potential of ROS and antioxidants.

Redox couple	E^0/V
$\text{OH}^\cdot, \text{H}^+ / \text{H}_2\text{O}$	2.33
$\text{OCl}^\cdot, 2\text{H}^+ / \text{Cl}^\cdot, \text{H}_2\text{O}$	1.49
$\text{ONOO}^\cdot, 2\text{H}^+ / \text{NO}_2^\cdot, \text{H}_2\text{O}$	1.4
$\text{O}_2^\cdot, 2\text{H}^+ / \text{H}_2\text{O}_2$	0.94
$\text{H}_2\text{O}_2, \text{H}^+ / ^\cdot\text{OH}, \text{H}_2\text{O}$	0.38
$\text{NO}_2^\cdot, \text{H}_2\text{O} / \text{NO}, 2\text{OH}^\cdot$	−0.46
$\text{C}_2\text{O}_4^{2-} / 2\text{CO}_2$	−0.59
$\text{BH}_4^-, 8\text{OH}^- / \text{H}_2\text{BO}_3^-, 5\text{H}_2\text{O}$	−1.24